Segmentation of Carotid Arteries By Graph-Cuts Using Centerline Models

M. Akif Gülsün, Hüseyin Tek

September 23, 2009

Imaging and Visualization Department, Siemens Corporate Research, Princeton, NJ 08540

Abstract

In this paper, we present a semi-automatic method for segmenting carotid arteries in contrast enhanced (CE)-CT angiography (CTA) scans. The segmentation algorithm extracts the lumen of carotid arteries between user specified locations. Specifically, the algorithm *first* detects the centerline representations between the user placed seed points. This centerline extraction algorithm is based on a minimal path detection algorithm which operates on a *medialness* map. The lumen of carotid arteries is extracted by using the global optimal graph-cuts algorithm [4] using centerlines as input. The distance from the centerline representation is used to normalize the gradient based weights of the graph. It is shown that this algorithm can sucessfully segment the carotid arteries without including calcified and non-calcified plaques in the segmentation results.

Contents

1 Centerline Extraction of Carotid Arteries **2**
1.1 Medialness Measure From 2D Cross-Sectional Models 2
1.2 Centerline Extraction Betwen Seed Points 3

2 Graph-Cuts Using Centerlines for Lumen Extraction **5**

3 Results **7**

Segmentation of carotid arteries in CTA is often a necessary task for obtaining stenosis measurements, stent planning and advanced visualization. There are numerous segmentation algorithms ranging from simple thresholding and region growing to more complex deformable models techniques starting from centerline models obtained directly from images, etc, *e.g.*, [7, 18, 16, 1, 8, 13, 10, 22, 3, 2, 21, 6]. In general, the timely and robust segmentation of carotid arteries is still a difficult task due to the existence of plaques (calcified and non-calcified) on the vessel wall and the presence of nearby veins and bones.

In this paper, we present a semi-automatic segmentation algorithm for extracting the lumen of carotid arteries in CE-CTA data. This algorithm requires three seed placement to select the vessel of the interest[1] The proposed algorithm is based on the global graph-cut optimization algorithm [4] using vessel centerlines

[1] Single click carotid segmentation is also possible with the modified version of the algorithm [11].

extracted between the user placed seed points via [11]. In general, the graph-cuts algorithms are not suitable for segmenting elongated shapes such as blood vessels since the minimum energy surfaces often do not coincide with the boundaries of vessels. In this paper, we show that the integration of vessel centerlines makes the graph-cuts algorithm to be sucessfully used for the segmentation of vessels. Specifically, centerlines are important for three main reasons: (i) foreground seeds required by the graph-cuts algorithm are obtained from the location of centerlines. (ii) the weights of discrete graph edges are normalized by the distance from the centerline representations. (iii) the global optimization is limited to the vicinity of centerline by constructing a tubular graph for computational reasons and robustness. This algorithm is implemented by using the "max-flow" algorithm [5].

This paper is organized as follows as: In Section 1, we describe the centerline extraction algorithm which is based on minimal path detection. Specifically, we first explain the multi-scale medialness filters (Section1.1) which are used in the centerline tracking algorithm. The centerline extraction algorithm is described for a centerline segment between source and sink seeds in Section1.2. In Section 2, we describe the global graph-cuts algorithm using centerlines for extracting carotid lumens. Finally, Section3 presents some results.

1 Centerline Extraction of Carotid Arteries

We first summarize the framework for the extraction of center-axis representation of vessels from CTA which is also applicable to vessels found in MRA and 3D-X ray. Specifically, first, a *medialness* measure based on 2D multi-scale cross-sectional models is introduced. This measure is contrast and scale independent and it works well in the presence of nearby bright structures such as bones or other vessels. Second, we present a minimal path detection method working on a discrete grid where the cost of graph edges are computed from multi-scale medialness filters. This algorithm can be used to extract the the full vessel centerline tree from a single seed by a post-processing algorithm which uses the length and scale of vessel centerlines. In general, the proposed method can produce centerline model(s) for a vessel segment and the full vessel tree. In addition, it is capable of capturing different size of vessel branches, crossing over stenosis. Moreover, it is computationally efficient. Let us now describe the algorithm in more detail:

1.1 Medialness Measure From 2D Cross-Sectional Models

We describe a technique for computing medialness measure which is based on multi-scale cross-sectional vessel modeling. Blood vessels in CTA/MRA have typically circular/elliptic shapes in cross-sectional views even though local variations on them are not too uncommon due to the presence of nearby vessels or pathologies. Ideally, a 2D cross-sectional vessel profile consists of a circular/elliptic bright disk and darker ring around it. Our medialness measure uses this circularity assumption and edge responses obtained from multi-scale filters. Specifically, our medialness response, $m(\vec{x_0})$ at $\vec{x_0}$, is computed from a circle $C(\vec{x_0},R)$ centered at $\vec{x_0}$, with radius R, and is given by

$$m(\vec{x_0}) = \max_R \{\frac{1}{N}\sum_{i=0}^{N-1} E(\vec{x_0} + Ru(2\vec{\pi i}/N))\} \quad (1)$$

where $\vec{u}(\alpha) = sin(\alpha)\vec{u_1} + cos(\alpha)\vec{u_2}$ and $\vec{u_1}$ and $\vec{u_1}$ defines a 2D plane. E measures the normalized edge response which is described below. Krissian *et. al.*, [14] proposed a similar medialness measure where the cross-sectional plane is computed from the eigenvectors of Hessian matrix.

Let us consider a 1-D intensity profile $I(x)$ along a ray $\vec{u_\alpha}$ on a cross-sectional plane of a vessel starting from the location $\vec{x_0}$. Suppose that $\vec{x_0}$ is the center of the vessel with a radius R. Then the cross-sectional boundary

of the vessel along the ray should occur at $(\vec{x_0}+R\vec{u_\alpha})$ where the gradient of $I(x)$ has a maxima and the second derivative of $I(x)$ has a zero-crossing. We propose to use the gradient, $\nabla_\sigma I(x)$ for measuring responses at vessel boundaries, in which σ corresponds to the spatial scale of the vessel boundary. In general, filter sizes are often selected from the size of vessels for computing gradient responses [14], *i.e.*, larger spatial filters for large vessels. It should be noted that vessel scale, namely R and boundary scale, σ are not always related. For example, the boundary of a large vessel can be detected *better* with small size filters when such vessels are surrounded by other bright structures. Similarly, it is possible that small scale vessels can have long diffused boundaries which cannot be accurately detected via small scale filters.

Let us now define the boundary measure along a ray $\vec{u_\alpha}$ at the location x,

$$b(x) = \max_\sigma\{(|\nabla_\sigma I(x)|)\}sign(\nabla_\sigma I(x)) \tag{2}$$

where $sign(x)$ is used to distinguish the rising (dark to bright changes) and falling edges (bright to dark changes). Observe that this boundary measure, $\nabla_\sigma I$ is contrast dependent, *i.e.*, it obtains higher values from high contrast vessels and lower values from low contrast vessels, respectively. Unfortunately, vessels may have significant intensity variations on them - especially vessels in MRA and small size vessels in CTA. In addition, boundaries of bones, calcifications in CTA and vessels next to airways can have strong gradients which usually effect the response of medialness filters. We, in fact, believe that medialness responses should be contrast independent, which can be accomplished by normalizing the boundary measure via the highest gradient obtained for different R values along the ray. Mathematically, we define a normalized boundary measure as $\hat{b}(x) = b(x)/b_{max}$ where b_{max} is the maximum falling edge response along $I(x)$ for $x = \{\vec{x_0}+R_{min}\vec{u_\alpha},..,\vec{x_0}+R_{max}\vec{u_\alpha}\}$ and R_{min} and R_{max} are the minimum and maximum vessel scales, respectively.

Since the size of vessels to be modeled is not known a priori, our method searches for strong edge responses at the different locations along the ray u_α with different R, $R \in [R_{min}, R_{max}]$. However, observe that for large values of R this produces strong boundary responses at locations which are outside the vessel. In general, there should not be any strong rising edge between $\vec{x_0}$ and $\vec{x_0}+R\vec{u_\alpha}$ where the boundary is searched. If there exists such a strong rising edge, it probably means that the point $\vec{x_0}$ is outside the vessel, thus it should have a lower medialness measure. This is accomplished by first computing the maximum rising boundary response up to the location $\vec{x_0}+R\vec{u_\alpha}$ along the ray and then subtracting this value from the response obtained at $\vec{x_0}+R\vec{u_\alpha}$. Based on these modifications, the final edge response along a ray, $\vec{u_\alpha}$, starting from at $\vec{x_0}$, $E(\vec{x_0}+R\vec{u_\alpha})$ is given as

$$E(\vec{x_0}+R\vec{u_\alpha}) = \frac{\max(-b(\vec{x_0}+R\vec{u_\alpha}) - \min_{x\in\{\vec{x_0},\vec{x_0}+R\vec{u_\alpha}\}}(b(x),0),0)}{max_{x\in(\vec{x_0}+R_{min}\vec{u_\alpha},\vec{x_0}+R_{max}\vec{u_\alpha})}(-b(x),1)} \tag{3}$$

The proposed medialness measure gives strong responses at the center of a vessel and responses drop rapidly towards vessel boundaries and very small responses are obtained in non-vascular areas, Figure1. Also, the presence of bright structures does not have strong impact on the responses.

1.2 Centerline Extraction Betwen Seed Points

In this section, we describe a method for extracting local center axis representations by integrating the medialness map in a discrete optimization framework. Specifically, we seek to obtain a curve $C(s)$ (center axis) between points p_0 and p_1 which travels through the center of a vessel. This problem can be successfully solved by the *minimum-cost* path detection algorithms [8, 15, 20]: Let $E(C)$ be the total energy along a curve C

$$E(C) = \int_\Omega (P(C(s)) + w)ds \tag{4}$$

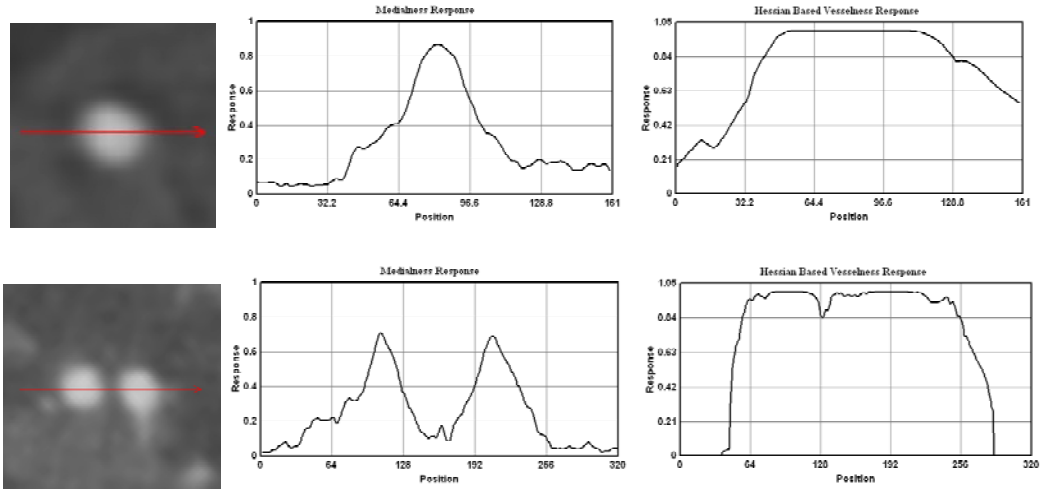

Figure 1: This figure illustrates the medialness responses along a ray on two different examples obtained from our method (middle column) and the Hessian-based method (right column). Observe that unlike Hessian based methods, our technique gives low responses between two nearby vessels.

where $P(C)$ is called potential, w is the regularization term and s is the arch length, *i.e.*, $||C(s)|| = 1$. In vessel centerline extraction methods, potential $P(x)$ at x corresponds to the inverse of a medialness measure at that location, namely, $P(x) = \frac{1}{m(x)}$. Let A_{p_0,p_1} represents the set of all curves between p_0 and p_1. The curve with total minimum energy can be computed from the *minimum-accumulative cost*, $\phi(p)$ which measures the minimal energy at p integrated along a curve starting from the point p_0:

$$\phi(p) = \inf_{A_{p_0,p_1}} \{E(C)\} \tag{5}$$

This type of minimization problems has been studied extensively in computer vision for different problems, *e.g.*, segmentation. They are usually solved by either Dijkstra's algorithm [9] or Fast Marching methods [17]. In this paper, we propose to use Dijkstra's algorithm for solving equation (5) in a discrete domain. Specifically, let $G = (N,E)$ be a discrete graph where N and E represent nodes and edges, respectively. The minimum-accumulative cost at the node P_{ij} for a four connected 2D graph is then given by

$$\phi(P_{ij}) = min(\phi(P_{i-1j}) + C^{ij}_{(i-1)j}, \phi(P_{i+1j}) + C^{ij}_{(i+1)j}, \phi(P_{ij-1}) + C^{ij}_{i(j-1)}, \phi(P_{ij+1}) + C^{ij}_{i(j+1)}) \tag{6}$$

where, for example, $C^{ij}_{(i-1)j}$ corresponds to the cost of propagation from point $P_{(i-1)j}$ to P_{ij} which is obtained from the inverse of medialness measure. This above algorithm can be easily implemented by first setting minimum-accumulative cost of all nodes to infinity (or a large value) and then using an explicit discrete front propagation method where propagation always takes places from the minimum value to its neighboring nodes. In our implementation, we use 26-connected lattice in 3D, *i.e.*, diagonal propagations are also included for better accuracy. In addition, the medialness measure is computed orthogonal to the direction of propagation instead of computing at nodes. The discrete path (curve) from a point P_{ij} to source P_0 can then be easily obtained by traversing (backtracking) along the propagation. This algorithm works well even in the presence of nearby vessels, strong calcification and strong contrast change along a vessel and it is computationally efficient. Figure 2 illustrates some results obtained from this algorithm.

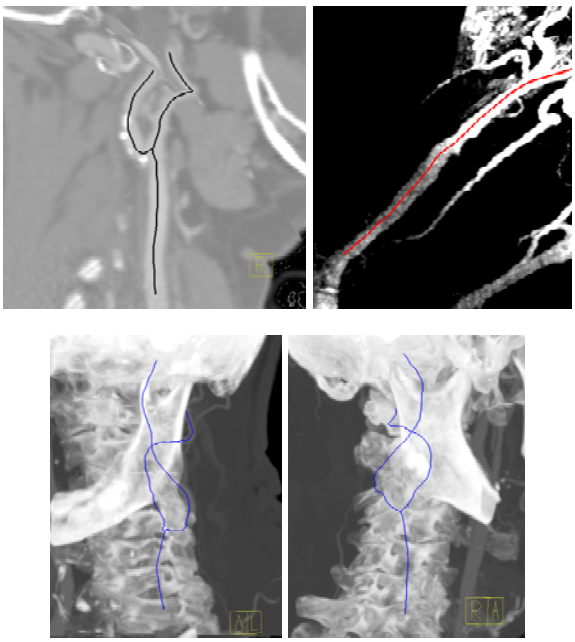

Figure 2: This figure illustrates the centerlines extracted betwen user placed seed points by the proposed algorithm.

2 Graph-Cuts Using Centerlines for Lumen Extraction

In this section, we propose a novel method for extracting the lumen of carotid arteries in CTA by using the centerlines detected between the user placed seed points. Specifically, we propose to use the global optimal graph-cuts algorithm [4] to extract the vessel boundaries given the detected foreground seed-points from the centerlines. In general, graph-cuts typically does not perform well in segmenting elongated shapes such as blood vessels because it often tends to be biased towards shorter boundaries. Our proposed method, however, solves the shrinking problem for the case of blood vessels by using the centerlines as input to the graph-cut algorithm and adjusting the weights of the graph via centerlines.

Let us now summarize the graph-cuts algorithm: Let G = (P, N) be a graph with a set of nodes P and undirected edges N that connect these nodes. In this graph, each edge is assigned with a nonnegative weight (cost) w_e. The graph-cuts generally minimizes a global energy function

$$E(f) = \lambda \sum_{p \in P} R_p(A_p) + \sum_{(p,q) \in N} B_{pq} \gamma(A_p, A_q) \tag{7}$$

where

$$\gamma(A_p, A_q) = \begin{cases} 1 & \text{if } A_p \neq A_q \\ 0 & \text{else} \end{cases} \tag{8}$$

where A_p specifies assignments to pixels in P. Specifically, each pixel p is either assigned to be "background" or "foreground". The first term in the global energy function, $E(f)$ defines the regional properties of the segmentation. Similarly, the second term comprises the boundary properties of the segmentation. In our carotid segmentation problem, we do not use the regional term, *i.e.*, $\lambda = 0$, Then, the boundary of carotid arteries can be viewed as a surface where the total boundary energy is minimal. However, the direct application of this graph cuts segmentation algorithm to our problem may not be appropriate since the minimum energy surface can consist of few voxels which then may not correspond to the carotid boundaries. In other words, the minimum energy surface is size dependent and incorrect alignment of small number of voxels can produce a surface with the minimum energy.

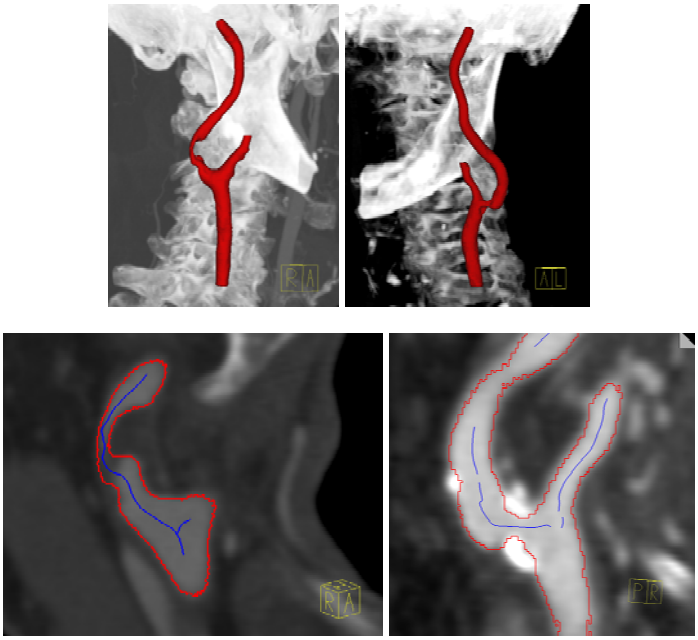

Figure 3: This figure illustrates the results of carotid artery segmentation from our algorithm.

Thus, we propose the following modifications to the graph-cuts algorithm to make it more suitable for blood vessel segmentation. (1) A tubular graph construction in the vicinity of centerlines is proposed. This allows the global minimization algorithm converge faster and provide more robust results since it includes the minimum amount of nearby structures such as bones or veins. (2) Extracted centerline points are marked as the source and similarly, the outer surface voxels of the tubular mask are marked as the sinks. (3) The image gradients that are used in the weights of the graph edges are computed orthogonal to the centerline. This makes gradients are more robust to noise. In addition, the notion of rising and falling gradients are integrated to the algorithm by using rays connecting graph edges to the closest points on the centerline. Specifically, significant rising edge before any falling edge signals the presence of an edge from a calcified plaque. In this case, the falling gradients is set to small value since lumen cannot include calcified plaques. Moreover, advanced gradient computations such as mean-shift based edge detection [19] are possible along a ray starting from the centerline and intersecting edges of the graph. (4) The weights of the edges are normalized by the distance from the centerlines to assign higher weights to the edges that are closer to the centerlines and lower weights to the edges that are away from the centerlines since surface closer to the centerline contain fewer number of voxels. Thus, this new weight computation allows the algorithm to be more independent from the size of resulting surface.

The centerline based graph cuts algorithm is then implemented by using the "max-flow" algorithm introduced by Boykov [5]. We first detect the centerline between common carotid artery (CCA) and internal carotid artery (ICA) and the lumen is extracted with the proposed graph-cut algorithm. Similarly, the same approach is taken between CCA and the external carotid artery (ECA). The final carotid artery mask is obtained by taking the union of these maks. This independent segmentation of each branch was important to obtain smooth segmentation in the vicinity of the branch. Figure 3 illustrates some of the results obtained from this algorithm.

Table 1: Summary lumen

Measure	% / mm			rank		
	min.	max.	avg.	min.	max.	avg.
L_dice	80.4%	95.5%	92.3%	3	4	3.97
L_msd	0.08mm	0.48mm	0.17mm	3	4	3.97
L_rmssd	0.11mm	0.77mm	0.24mm	3	4	3.97
L_max	0.44mm	3.37mm	1.09mm	3	4	3.81
Total (lumen)				**3**	**4**	**3.93**

Table 2: Averages lumen

Team name	Total success	dice		msd		rmssd		max		Total rank
		%	rank	mm	rank	mm	rank	mm	rank	
SCR_Gulsun_Tek	31	92.3	4.0	0.17	4.0	0.24	4.0	1.09	3.8	3.9
ObserverA	31	95.4	1.5	0.10	1.5	0.13	1.6	0.56	1.9	1.6
ObserverB	31	94.8	2.4	0.11	2.4	0.15	2.3	0.59	1.8	2.2
ObserverC	31	94.7	2.2	0.11	2.2	0.15	2.1	0.71	2.5	2.2

3 Results

The method was evaluated on the 31 CTA datasets of the Testing set of the challenge [12]. Quantitative results are given in Tables 1 and 2.

The quality of results are visually inspected by overlaying them on the original images. We have observed that calcified plaques are often successfully removed from the plaques. However, our results still require some improvements around branch points. This is especially true when smaller branches are not modeled by centerlines. Specifically, we observed that small amount of region from the other branches are included in the carotid mask. These errors often result in large maximum errors.

We emphasize the computational efficiency of our approach. Such a criterion is absent from the challenge evaluation but is, in our opinion, essential for the clinical applicability of the method. Semi-automatic segmentation of carotid lumen can be achieved in less than 50 seconds where centerline extraction part takes less than 20 seconds and surface modeling part takes less than 30 seconds. In addition, the lumen of carotid arteries can be easily detected with a single seed placement instead of three seeds provided to be used in the challenge since our centerline extraction algorithm can detect vessel centerline tree. Furthermore, our framework provides the user with simple tools for correcting and extending results at nearly interactive speeds.

References

[1] Briant B. Avants and James P. Williams. An adaptive minimal path generation technique for vessel tracking in CTA/CE-MRA volume images. In *Medical Image Computing and Computer-Assisted Intervention MICCAI*, pages 707–716, 2000. (document)

[2] S. Aylward and E. Bullitt. Initialization, noise, singularities, and scale in height-ridge traversal for tubular object centerline extraction. *TMI*, 21(2):61–75, 2002. (document)

[3] S. Aylward, S. Pizer, E. Bullitt, and D. Eberly. Intensity ridge and widths for 3d object segmentation and description. In *IEEE Proc. Workshop MMBIA*, pages 131–138, 1996. (document)

[4] Y. Boykov and M.P. Jolly. Interactive graph cuts for optimal boundary and region segmentation of objects in N-D images. In *International Conference Computer Vision*, volume I, pages 105–112, 2001. (document), 2

[5] Yuri Boykov and Vladimir Kolmogorov. An experimental comparison of min-cut/max-flow algorithms for energy minimization in vision. *IEEE Trans. Pattern Anal. Mach. Intell.*, 26(9):1124–1137, 2004. (document), 2

[6] J. Chen and A. A. Amini. Quantifying 3-d vascular structures in mra images using hybrid pde and geometric deformable models. *IEEE Transactions on Medical Imaging*, 23:1251–1262, 2004. (document)

[7] A. Chung and J. A. Noble. Statistical 3D vessel segmentation using a Rician distribution. In *MICCAI*, pages 82–89, 1999. (document)

[8] T. Deschamps and L.D. Cohen. Fast extraction of minimal paths in 3d images and applications to virtual endoscopy. *Medical Image Analysis*, 5(4):281–299, 2001. (document), 1.2

[9] E. W. Dijkstra. A note on two problems in connections with graphs. *Numerische Mathematic*, 1:269–271, 1959. 1.2

[10] A. F. Frangi, W. J. Niessen, K. L. Vincken, and M. A. Viergever. Multiscale vessel enhancement filtering. In *MICCAI*, pages 82–89, 1998. (document)

[11] M. A. Gulsun and H. Tek. Robust tree modeling. In *MICCAI*, 2008. 1, (document)

[12] K. Hameeteman, M. Zuluaga, L. Joskowicz, M. Freiman, and T. vanWalsum. 3d segmentation in the clinic: Carotid lumen segmentation and stenosis grading challenge. 2009.http://cls2009.bigr.nl. 3

[13] T. M. Koller, G. Gerig, and G. Szekely an D. Dettwiler. Multiscale detection of curvilinear structures in 2-d and 3-d image data. In *ICCV*, pages 864–869, 1995. (document)

[14] K. Krissian, G. Malandain, N. Ayache, R. Vaillant, and Y. Trousset. Model based multiscale detection of 3d vessels. In *IEEE Conf. CVPR*, pages 722–727, 1998. 1.1

[15] Hua Li and Anthony J. Yezzi. Vessels as 4-d curves: Global minimal 4-d paths to extract 3-d tubular surfaces and centerlines. *IEEE Trans. Med. Imaging*, 26(9):1213–1223, 2007. 1.2

[16] D. Nain, A. Yezzi, and Greg Turk. Vessel segmentation using a shape driven flow. In *MICCAI*, 2004. (document)

[17] J. A. Sethian. *Level Set Methods*. Cambridge University Press, New York, 1996. 1.2

[18] K. Siddiqi and A. Vasilevskiy. 3d flux maximizing flows. In *International Workshop on Energy Minimizing Methods In Computer Vision*, 2001. (document)

[19] H. Tek, A. Ayvaci, and D. Comaniciu. Multi-scale vessel boundary detection. In *Workshop of CVBIA*, pages 388–398, 2005. 2

[20] James Alexander Tyrrell, Emmanuelle di Tomaso, Danel Fuja, Ricky Tong, Kevin Kozak, Edward B. Brown, Rakesh Jain, and Badrinath Roysam. Robust 3-d modeling of vasculature imagery using superellipsoids. *IEEE Transactions on Medical Imaging*, 2006. 1.2

[21] Cornelis M. van Bemmel, Luuk J. Spreeuwers, Max A. Viergever, and Wiro J. Niessen. Level-set based artery-vein separation in blood pool agent ce-mr angiograms. *IEEE Trans. Med. Imaging*, 22(10):1224–1234, 2003. (document)

[22] O. Wink, W. J. Niessen, and M. A. Viergever. Multiscale vessel tracking. *IEEE Trans. on Medical Imaging*, 23(1):130–133, 2004. (document)